Ferroelectricity in Spiral Magnets

Maxim Mostovoy

Materials Science Center, University of Groningen, Nijenborgh 4, 9747 AG Groningen, The Netherlands
II Physikalisches Institut, Universität zu Köln, Zülpicherstrasse 77, D-50937 Köln, Germany

(Received 26 October 2005; published 15 February 2006)

It was recently observed that the ferroelectrics showing the strongest sensitivity to an applied magnetic field are spiral magnets. We present a phenomenological theory of inhomogeneous ferroelectric magnets, which describes their thermodynamics and magnetic field behavior, e.g., dielectric susceptibility anomalies at magnetic transitions and sudden flops of electric polarization in an applied magnetic field. We show that electric polarization can also be induced at domain walls and that magnetic vortices carry electric charge.

DOI: 10.1103/PhysRevLett.96.067601 PACS numbers: 77.80.Fm, 75.30.Fv, 75.60.Ch

Effective interactions of charges and spins in solids are often quite different from the fundamental laws of electrodynamics, which gives rise to unusual phenomena. The coupling between static electric and magnetic dipoles, observed in multiferroic materials, is a fascinating effect interesting both for its fundamental physics and potential technological applications [1,2]. Like colossal magnetoresistance, it involves interplay between charge, spin, orbital, and lattice degrees of freedom.

Many known multiferroics, e.g., $BiFeO_3$, are essentially ferroelectrics with magnetic ions, in which spins order at much lower temperatures than electric dipoles and effect of magnetic transition on dielectric constant is weak. The search for strongly coupled magnetism and ferroelectricity recently led to a discovery of a new class of materials, e.g., rare earth manganites $TbMnO_3$, $DyMnO_3$, and $TbMn_2O_5$ [3–8], in which electric polarization is only observed in magnetically ordered states. These ferroelectric magnets exhibit an exceptionally strong sensitivity to an applied magnetic field, which induces reversals and sudden flops of the electric polarization vector [4,6,8], and results in a strong enhancement of dielectric constant (the giant magnetocapacitance effect) [5].

This level of control of dielectric properties by magnetism is only possible because electric polarization in these materials is induced by magnetic ordering. The onset of ferroelectricity correlates with the transition to a spiral spin-density-wave (SDW) state. Periodically modulated magnetic structures in insulators result from competing exchange interactions [3] and are often found in so-called geometrically frustrated materials [9], such as the ferroelectric Kagomé magnet $Ni_3V_2O_8$ [10]. The link between ferroelectricity and magnetic frustration is an intriguing feature of the new class of multiferroics.

In this Letter we obtain a simple expression for electric polarization induced by incommensurate SDW states. We apply the Ginzburg-Landau approach to thermodynamics and magnetic field behavior of ferroelectric magnets and, in particular, discuss anomalies in dielectric constant at magnetic transitions and electric polarization flops in magnetic field. This phenomenological approach, based on symmetry considerations, is complementary to the recent discussions of microscopic mechanisms of ferroelectricity in magnets [11,12].

Induced polarization.—Incommensurate SDW states are largely insensitive to details of crystal structure and can be described by a continuum field theory of the Ginzburg-Landau type. The form of the coupling of the electric polarization $\mathbf{P}$ to the magnetization $\mathbf{M}$ can be found using general symmetry arguments [13]. The invariance upon the time reversal, $t \to -t$, which transforms $\mathbf{P} \to \mathbf{P}$ and $\mathbf{M} \to -\mathbf{M}$, requires the lowest-order coupling to be quadratic in $\mathbf{M}$. The symmetry with respect to the spatial inversion, $\mathbf{x} \to -\mathbf{x}$, upon which $\mathbf{P} \to -\mathbf{P}$ and $\mathbf{M} \to \mathbf{M}$, is respected when the coupling of a uniform polarization to an inhomogeneous magnetization is linear in $\mathbf{P}$ and contains one gradient of $\mathbf{M}$.

The coupling linear in gradient of an order parameter, called Lifshitz invariant (LI), is allowed in systems with broken inversion symmetry, such as noncentrosymmetric crystals, where it can give rise to periodic modulations of magnetization [13]. Such an incommensurate SDW state is observed in the ferroelectric $BiFeO_3$, where the inversion symmetry is spontaneously broken by electric polarization. Here the LI, describing the coupling between $\mathbf{P}$ and the Néel vector $\mathbf{L}$, induces a spiral magnetic ordering, in which $\mathbf{L}$ rotates with the period 620 Å [14]. The small value of the wave vector is a consequence of the relativistic nature of the coupling [13,15].

This reasoning can be turned around to explain electric polarization in frustrated magnets, in which an incommensurate magnetic ordering results from competing exchange interactions and the SDW wave vector is, in general, not small. When the SDW order of a proper kind sets in, the coupling of the LI type induces a uniform electric polarization that breaks the inversion symmetry. The weakness of the coupling translates in this case to relatively low values of the induced polarization.

This mechanism does not require a special kind of crystal lattice. In the simplest case of cubic symmetry the

coupling term has the form

$$\Phi_{em}(\mathbf{P}, \mathbf{M}) = \gamma \mathbf{P} \cdot [\mathbf{M}(\nabla \cdot \mathbf{M}) - (\mathbf{M} \cdot \nabla)\mathbf{M} + \cdots]. \quad (1)$$

The omitted terms can be written as the total derivative, $\nabla f(\mathbf{M})$, and do not contribute to the uniform polarization. Assuming that in absence of magnetism the system shows no instability towards ferroelectricity, we only keep the quadratic term in the "electric part" of thermodynamic potential, $\Phi_e(\mathbf{P}) = \frac{P^2}{2\chi_e}$, where χ_e is the dielectric susceptibility in absence of magnetism. The variation of $\Phi_e + \Phi_{em}$ with respect to $\mathbf{P}$ then gives

$$\mathbf{P} = \gamma \chi_e [(\mathbf{M} \cdot \nabla)\mathbf{M} - \mathbf{M}(\nabla \cdot \mathbf{M})]. \quad (2)$$

Consider now a SDW state with the wave vector $\mathbf{Q}$,

$$\mathbf{M} = M_1 \mathbf{e}_1 \cos \mathbf{Q} \cdot \mathbf{x} + M_2 \mathbf{e}_2 \sin \mathbf{Q} \cdot \mathbf{x} + M_3 \mathbf{e}_3, \quad (3)$$

where the unit vectors $\mathbf{e}_i$, $i = 1, 2, 3$ form an orthogonal basis. If only M_1 or M_2 is nonzero, Eq. (3) describes a sinusoidal wave [see Fig. 1(a)], while for $M_1, M_2 \neq 0$ it describes an (elliptical) helix with the spin rotation axis $\mathbf{e}_3$ (if also $M_3 \neq 0$, the helix is conical). Using Eq. (2), we find that the average polarization is transverse both to $\mathbf{e}_3$ and $\mathbf{Q}$ [see Fig. 1(b)], and is independent of M_3:

$$\bar{\mathbf{P}} = \frac{1}{V} \int d^3x \mathbf{P} = \gamma \chi_e M_1 M_2 [\mathbf{e}_3 \times \mathbf{Q}]. \quad (4)$$

No average polarization is induced by a sinusoidal SDW, as the inversion symmetry at the sites where the magnetization reaches maximum or minimum [e.g., on the dashed line in Fig. 1(a)] remains unbroken. Equation (4) also holds for orthorombic crystals, provided that $\mathbf{e}_3$ and $\mathbf{Q}$ are parallel to crystal axes.

This explains why the transition at $T_S = 41$ K to the sinusoidal SDW state in $TbMnO_3$ [4,16] does not give rise to ferroelectricity and polarization is only induced below

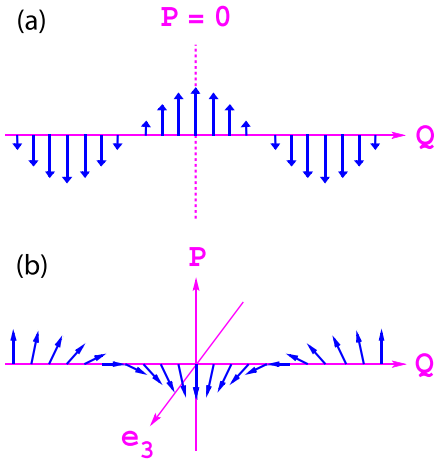

FIG. 1 (color online). The sinusoidal SDW (a) does not induce a uniform electric polarization; for a helicoidal SDW (b) $\mathbf{P}$ is orthogonal both to the spin rotation axis $\mathbf{e}_3$ and the wave vector $\mathbf{Q}$.

the so-called lock-in transition at $T_H = 28$ K, at which the sinusoidal SDW is replaced by the helix with $\mathbf{Q} \parallel b$. Since the Mn spins rotate in the bc plane ($\mathbf{e}_3 \parallel a$) [16], Eq. (4) gives $\mathbf{P} \parallel c$, in agreement with experiment. Similarly, the polarization is absent in the high-temperature incommensurate phase of $Ni_3V_2O_8$, which is the sinusoidal SDW state [10]. The helix with $\mathbf{Q} \parallel a$ and the spin rotation axis $\mathbf{e}_3 \parallel c$, observed in the low-temperature incommensurate phase, induces $\mathbf{P}$ along the b axis.

The spiral ordering is a particular case of two noncollinear SDWs with equal wave vectors, $\mathbf{M} = M_1 \mathbf{a}_1 \times \cos(\mathbf{Q} \cdot \mathbf{x} + \phi_1) + M_2 \mathbf{a}_2 \cos(\mathbf{Q} \cdot \mathbf{x} + \phi_2)$. Such an ordering was recently found in RMn_2O_5 [17,18]. Although a single sinusoidal SDW does not induce polarization, the interference between the two SDWs gives

$$\bar{\mathbf{P}} = \gamma \chi_e M_1 M_2 \sin(\phi_2 - \phi_1)[\mathbf{Q} \times [\mathbf{a}_1 \times \mathbf{a}_2]]. \quad (5)$$

Magnetic textures.—Equation (2) implies that electric polarization can also be induced by magnetic defects and inhomogeneous ground states stabilized by magnetostatic interactions, e.g., vortices in nanodiscs [19]. The integrated quantities, such as the total polarization per unit area of a domain wall (DW), only depend on topology of the spin textures. For a DW with collinear spins and the Bloch DW with spins rotating around the normal to the wall, the total polarization is 0, while the Néel DW, in which spins rotate around an axis parallel to the wall, $\mathbf{M} = M[\cos\phi(x_1)\mathbf{e}_1 + \sin\phi(x_1)\mathbf{e}_2]$, has a nonzero total polarization that depends on the total rotation angle:

$$\int_{-\infty}^{+\infty} dx_1 \mathbf{P} = \gamma \chi_e M^2 \mathbf{e}_2 [\phi(+\infty) - \phi(-\infty)]. \quad (6)$$

The polarization induced by DW networks can account for the anomalies in dielectric function observed in the reentrant phase of $HoMnO_3$ [20]. Using Eq. (2) one can also show that the vortex

$$\mathbf{M} = M[\cos(n\phi + \phi_0)\mathbf{e}_1 + \sin(n\phi + \phi_0)\mathbf{e}_2],$$

where $\phi = \arctan\frac{x_2}{x_1}$ and ϕ_0 is an arbitrary angle, has quantized electric charge located at the vortex core: $q_n = nq_1$, where $q_1 = 2\pi\gamma\chi_e M^2$ and n is the winding number of the vortex. An applied electric field will pull magnetic vortices and antivortices in opposite directions.

Sinusoidal-helicoidal transition.—We now turn to the phase diagram of ferroelectric SDW magnets. Using the values of the induced polarization ($10^2 - 10^3$ $\mu C\,m^{-2}$) and magnetic transition temperatures (5–40 K) for these materials, we find that the energy gain due to the induced polarization is small compared to the magnetic energy gain. Therefore, the temperature and magnetic field dependence of the polarization merely reflects the changes in magnetic ordering, which can be described using the Ginzburg-Landau thermodynamic potential

$$\Phi_m = \sum_{i=x,y,z} \frac{a_i}{2}(M_i)^2 + \frac{b}{4}M^4 + \frac{c}{2}\mathbf{M}\left(\frac{d^2}{dx^2} + Q^2\right)^2\mathbf{M}. \quad (7)$$

We assume that $a_x < a_y < a_z$ (easy axis along the x direction). The last term in Eq. (7) favors a periodic SDW ordering with the wave vector Q along the x axis.

A down-shift of the ferroelectric transition with respect to the magnetic one, found in all magnetic ferroelectrics, is a consequence of magnetic anisotropy. While for an isotropic system the ground state is a helix with a constant M, an anisotropic system first undergoes a transition to the sinusoidal SDW state with $\mathbf{M}$ along the easy axis, $\mathbf{M} = M_x\hat{x}\cos Qx$, at temperature T_S: $a_x(T_S) = 0$. As temperature is lowered and the amplitude of the order parameter grows, the system undergoes a second transition at some $T_H < T_S$ to the helicoidal state, $\mathbf{M} = M_x\hat{x}\cos Qx + M_y\hat{y}\sin Qx$, provided that the anisotropy parameter $\Delta = a_y - a_x$ is not too large. When the two transitions occur at close temperatures, the higher harmonics in the SDW state are small and the helix appears at $a_y = a_x/3$. For $a_x(T) = \alpha(T - T_S)$ we then obtain

$$T_H = T_S - \frac{3\Delta}{2\alpha}. \quad (8)$$

The average electric polarization only appears in the helicoidal state and for spins rotating in the xy plane and $\mathbf{Q} \parallel \mathbf{x}$ it is parallel to the y axis:

$$P_y = \alpha\gamma\chi_e Q\sqrt{(T_H - T)(T_S + \Delta/(2\alpha) - T)}. \quad (9)$$

Note that since $P_y \propto M_xM_y$ [see Eq. (4)], it has a square-root anomaly at the ferroelectric transition, even though it is not a primary order parameter. Furthermore, as in proper ferroelectrics, the dielectric constant ε_{yy} diverges at T_H and obeys "the 1/2 law" [21]:

$$\varepsilon_{yy} \approx \begin{cases} \frac{A}{T - T_H}, & \text{for } T > T_H, \\ \frac{A}{2(T_H - T)}, & \text{for } T < T_H, \end{cases} \quad (10)$$

where $A = 6\Delta(\gamma\chi_e Q)^2/(\alpha b)$. The magnetic contribution to ε_{yy} is nonzero in the sinusoidal state and its temperature derivative $\varepsilon'_{yy}(T)$ is discontinuous at $T = T_S$: $\varepsilon'_{yy}(T_S + 0) - \varepsilon'_{yy}(T_S - 0) = -\frac{(2\gamma\chi_e Q)^2}{b(T_S - T_H)}$.

Behavior in magnetic field.—The salient feature of ferroelectric magnets is the strong sensitivity of their dielectric properties to magnetic field, which can suppress electric polarization or change its direction [6,10]. We first discuss polarization flops in the model Eq. (7). In weak fields spins rotate in the easy xy plane, so that the spin rotation axis $\mathbf{e}_3$ is parallel to the "hard" z axis, and for $\mathbf{Q} \parallel \mathbf{x}$, $\mathbf{P} \parallel \mathbf{y}$. In strong magnetic fields spins form a conical helix with $\mathbf{e}_3 \parallel \mathbf{H}$; e.g., H_x will force the spins to rotate in the zy plane [see Fig. 2(a)]. Such a spin flop suppresses electric polarization, since for the zy helix $\mathbf{e}_3 \parallel \mathbf{Q}$ and according to Eq. (4) $\mathbf{P} = 0$. On the other hand, magnetic field in the y direction favors the rotation of spins in the xz plane, in which case $\mathbf{P} \parallel \mathbf{z}$ [see Fig. 2(b)].

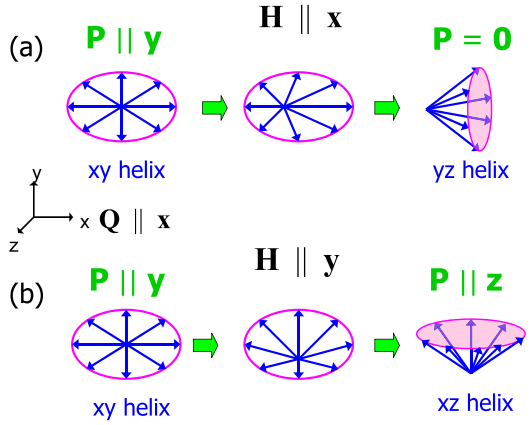

FIG. 2 (color online). Magnetic field behavior of electric polarization for the model Eq. (7). In zero field spins rotate in the xy plane and $\mathbf{P} \parallel \mathbf{y}$. Magnetic field in the x direction suppresses the polarization, while H_y orients $\mathbf{P}$ in the z direction.

The magnetic field behavior observed in orthorombic manganites is more involved. If we identify the x, y, and z axes in Eq. (7) with, respectively, the b, c, and a axes of the $Pbnm$ crystal structure of $TbMnO_3$, then magnetic field applied in the x and z directions changes the direction of $\mathbf{P}$ in $TbMnO_3$ from y to z. According to Eq. (4), this corresponds to the change of the rotation plane from xy to xz. It is the spin flop shown in Fig. 2(b), but induced by magnetic fields with "wrong" orientations.

This unusual behavior is most likely related to the flops of the strongly anisotropic rare earth spins, coupled to Mn spins [6,16]. It can be described phenomenologically by adding the higher-order anisotropies to Eq. (7), e.g.,

$$\Delta\Phi_m(\mathbf{M}) = b_{xy}(M_x)^2(M_y)^2 + b'_{xy}(M_x)^2\left(\frac{dM_y}{dx}\right)^2 + b_{yz}(M_y)^2(M_z)^2. \quad (11)$$

For $b_{xy}, b'_{xy}, b_{yz} > 0$ the first two terms suppress the rotation in the xy plane, when magnetic field is applied in the x or y direction, while the last term suppresses the rotation in the yz plane. This gives rise to phase diagrams, shown in Fig. 3, which are similar to those of $TbMnO_3$ [6]. The magnetic field dependence of the spin-flop temperature and the divergency of dielectric constant at T_H makes ε strongly field dependent [5].

Importantly, magnetic fields required to flop spins can be low for materials with small magnetic anisotropies containing magnetic ions with filled and half-filled t_{2g} shells. This opens a possibility to observe polarization flops in magnets with high transition temperatures, which may be interesting for applications. Consider, e.g., a *gedanken* experiment on the helimagnet $CaFeO_3$ with $T_N = 115$ K [22]. In zero field both the wave vector and spin rotation axis of the helix are parallel to the body diagonal, $\mathbf{Q}, \mathbf{e}_3 \parallel [1, 1, 1]$, and no electric polarization is expected. The field

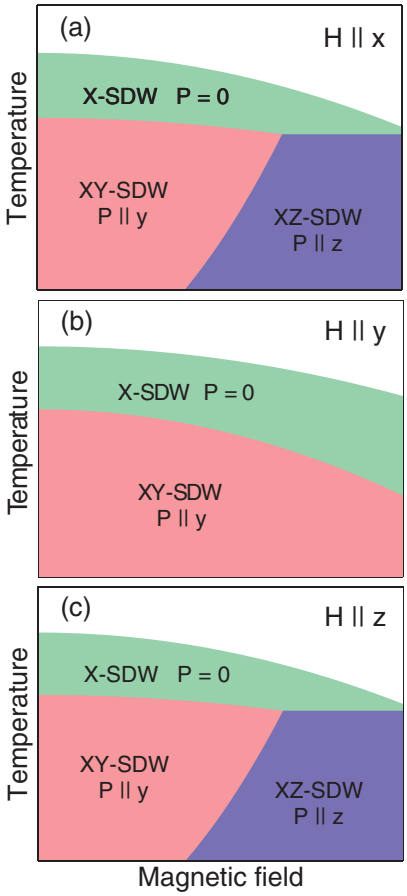

FIG. 3 (color online). Typical phase diagrams of the model Eq. (7) with nonlinear terms Eq. (11) included for $\mathbf{H} \parallel \mathbf{x}, \mathbf{y}, \mathbf{z}$ [respectively, panels (a), (b), and (c)]. Here X-SDW (green) denotes the sinusoidal SDW state with spins along the x axis, while XY-SDW (pink) and XZ-SDW (blue) denote the spiral states with spins rotating, respectively, in the xy and xz planes.

required to align $\mathbf{e}_3$ along $\mathbf{H}$ is much lower than the field that can change the orientation of $\mathbf{Q}$ [the latter is of the order of the superexchange between the Fe spins [23]]. Thus magnetic field along the crystal axis, $\mathbf{H} = H_x[1, 0, 0]$, will induce $\mathbf{P} = P[0, -1, 1]$. The result of the numerical calculation of $P(H_x)$, using the model similar to Eq. (7), is shown in Fig. 4.

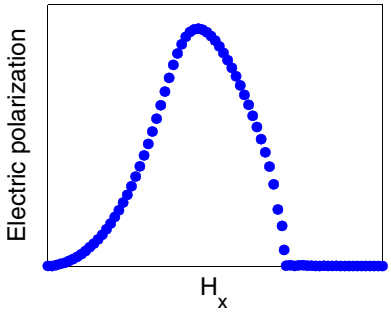

FIG. 4 (color online). Predicted magnetic field dependence of the electric polarization $|P^y| = |P^z|$ of $CaFeO_3$ for $\mathbf{H} \parallel \mathbf{x}$.

In conclusion, using symmetry arguments we showed that spiral magnets are, in general, ferroelectric. Electric polarization is also induced by Néel domain walls and magnetic vortices carry electric charge. We described phenomenologically magnetoelectric effects observed in spiral magnets, such as anomalies in dielectric constant at magnetic transitions and electric polarization flops induced by magnetic field, and discussed the possibility to observe these phenomena at high temperatures.

I would like to thank the University of Cologne for hospitality and Daniel Khomskii for numerous discussions. The financial support by the DFG and MSC^{plus} program is gratefully acknowledged.

[1] G. A. Smolenskii and I. E. Chupis, Sov. Phys. Usp. **25**, 475 (1982).
[2] M. Fiebig, J. Phys. D **38**, R123 (2005).
[3] T. Kimura, S. Ishihara, H. Shintani, T. Arima, K. T. Takahashi, K. Ishizaka, and Y. Tokura, Phys. Rev. B **68**, 060403(R) (2003).
[4] T. Kimura, T. Goto, H. Shintani, K. Ishizaka, T. Arima, and Y. Tokura, Nature (London) **426**, 55 (2003).
[5] T. Goto, T. Kimura, G. Lawes, A. P. Ramirez, and Y. Tokura, Phys. Rev. Lett. **92**, 257201 (2004).
[6] T. Kimura, G. Lawes, T. Goto, Y. Tokura, and A. P. Ramirez, Phys. Rev. B **71**, 224425 (2005).
[7] D. Higashiyama, S. Miyasaka, N. Kida, T. Arima, and Y. Tokura, Phys. Rev. B **70**, 174405 (2004).
[8] N. Hur, S. Park, P. A. Sharma, J. S. Ahn, S. Guha, and S-W. Cheong, Nature (London) **429**, 392 (2004).
[9] For reviews, see P. Schiffer and A. P. Ramirez, Comments Condens. Matter Phys. **18**, 21 (1996).
[10] G. Lawes *et al.*, Phys. Rev. Lett. **95**, 087205 (2005).
[11] I. E. Sergienko and E. Dagotto, cond-mat/0508075.
[12] H. Katsura, N. Nagaosa, and A. V. Balatsky, Phys. Rev. Lett. **95**, 057205 (2005).
[13] I. E. Dzyaloshinskii, Sov. Phys. JETP **10**, 628 (1960); **19**, 960 (1964).
[14] A. Kadomtseva, A. Zvezdin, Y. Popov, A. Pyatakov, and G. Vorob'ev, JETP Lett. **79**, 571 (2004).
[15] T. Morya, Phys. Rev. **120**, 91 (1960).
[16] M. Kenzelmann *et al.*, Phys. Rev. Lett. **95**, 087206 (2005).
[17] L. C. Chapon, G. R. Blake, M. J. Gutmann, S. Park, N. Hur, P. G. Radaelli, and S-W. Cheong, Phys. Rev. Lett. **93**, 177402 (2004).
[18] G. R. Blake, L. C. Chapon, P. G. Radaelli, S. Park, N. Hur, S-W. Cheong, and J. Rodríguez-Carvajal, Phys. Rev. B **71**, 214402 (2005).
[19] R. P. Cowburn, D. K. Koltsov, A. O. Adeyeye, M. E. Welland, and D. M. Tricker, Phys. Rev. Lett. **83**, 1042 (1999).
[20] T. Lottermoser and M. Fiebig, Phys. Rev. B **70**, 220407(R) (2004), and references therein.
[21] L. D. Landau and E. M. Lifshitz, *Electrodynamics of Continuous Media* (Pergamon, New York, 1975).
[22] S. Kawasaki, M. Takano, R. Kanno, T. Takeda, and A. Fujumori, J. Phys. Soc. Jpn. **67**, 1529 (1998).
[23] M. Mostovoy, Phys. Rev. Lett. **94**, 137205 (2005).